COMPACT SOLID-STATE WAVEGUIDE LASERS

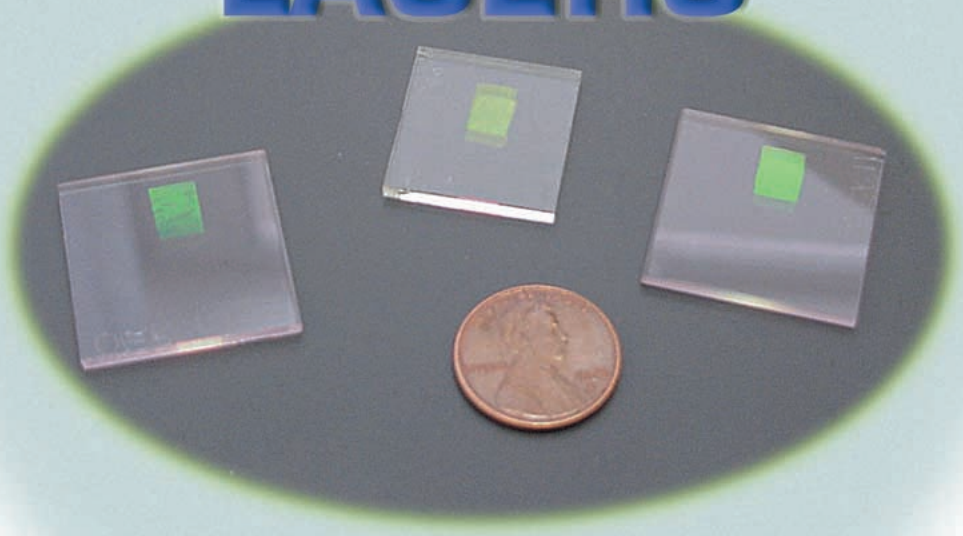

DBR and mode-locked Er/Yb waveguide lasers offer single-frequency and ultralow jitter performance.

By Berton E. Callicoatt, John B. Schlager, Robert K. Hickernell, Richard P. Mirin, and Norman A. Sanford

Glass waveguide lasers have an important niche in radio-frequency (RF) and microwave photonics, optical metrology, and telecommunications. This is primarily due to the compact size, low noise, relatively high output powers, and long upper-state lifetimes of these lasers. Waveguide lasers are also easily integrated into optical-fiber-based systems. Glass waveguide glass lasers share the same active medium as the more common erbium (Er)-doped fiber lasers (EDFLs) and amplifiers (EDFAs), but, unlike fiber-based devices, they are made with a thermally stable phosphate glass that is doped with much higher levels of Er. Waveguide lasers owe their compact size to the high-dopant concentration of the active rare-earth ions as well as low cavity loss. The concentration of rare-earth ions, such as Er and ytterbium (Yb), can be ten to 20 times higher in waveguide devices than in fiber-based lasers and amplifiers. This allows waveguide lasers and amplifiers to deliver higher output power in a smaller package and at lower cost than fiber-based devices. The compact, monolithic structure of waveguide lasers makes them ideal for use in mobile platform applications. Decreased cavity length in waveguide devices improves stability over fiber lasers by limiting the effects of environmental noise and decreases the need for isolation packaging. Waveguide amplifiers leverage these advantages in the metro telecommunications market, where compact, low-cost amplifiers with low noise and modest power (~10 dBm) are in demand. The shorter cavity length of

waveguide lasers is also an advantage in pulsed applications since, unlike fiber lasers, there is little or no need for dispersion compensation.

Glass waveguide lasers also compare favorably with semiconductor lasers; the long upper-state lifetime of the lasing transition in Er is on the order of milliseconds, which is much longer than the nanosecond lifetime found in semiconductor devices. This allows mode-locked waveguide lasers to operate with low noise at nearly any repetition rate above 1 MHz, whereas the gain stability in pulsed semiconductor lasers is perturbed by repetition rates lower than 1 GHz. Relaxation oscillations in semiconductor lasers occur at frequencies above 1 GHz, and their noise effects are not easily mitigated without high-speed control schemes. The lower frequency relaxation oscillations of glass waveguide lasers (less than 500 kHz) are more manageable. The low intracavity loss and relatively high output powers of the waveguide lasers lead to narrower linewidths than those of standard distributed feedback (DFB) semiconductor lasers. These same qualities enable ultralow jitter performance in passively mode-locked waveguide lasers. Waveguide lasers are easily coupled to optical-fiber-based systems with low coupling loss; this is an important advantage over bulk lasers, which are not easily integrated into fiber-optic systems.

Photonics applications for waveguide laser technology are numerous. Mode-locked waveguide lasers have applications in high-speed lightwave communications and in optical sampling systems for analog-to-digital (A-D) conversion of wide-band RF signals that require compact, low-jitter, pulsed lasers. They also can be used to optically distribute RF and microwave clock signals with high fidelity. Narrow-linewidth, single-frequency waveguide lasers have applications in metrology, remote sensing, and optical RF and microwave frequency generation.

Low intracavity loss and high output powers make both narrow-linewidth and ultralow-jitter waveguide lasers possible.

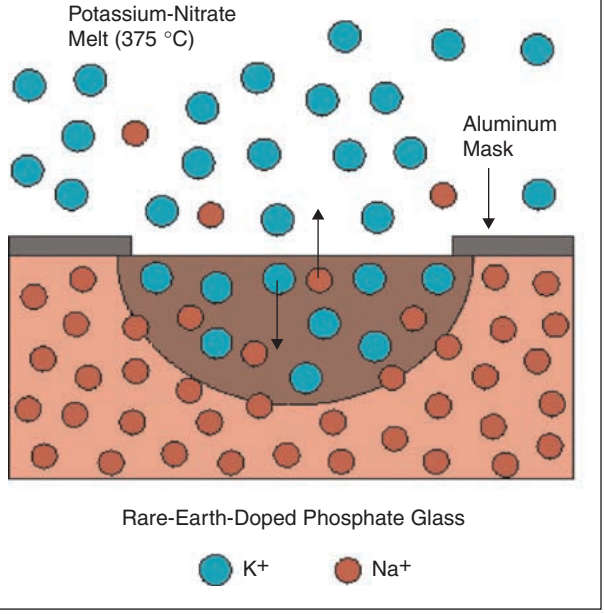

1. An illustration of the thermal ion exchange process. Refractive index features are formed when Na^+ ions in the Er/Yb codoped glass exchange with K^+ ions in the melt.

Optical Waveguide Fabrication in Er/Yb Codoped Phosphate Glass

The trick to forming optical waveguides is to cause refractive index changes in the substrate of the device that follow the pattern for a channel waveguide. There are a number of different methods to make these refractive index features and, thereby, fabricate optical waveguides in rare-earth-doped materials for

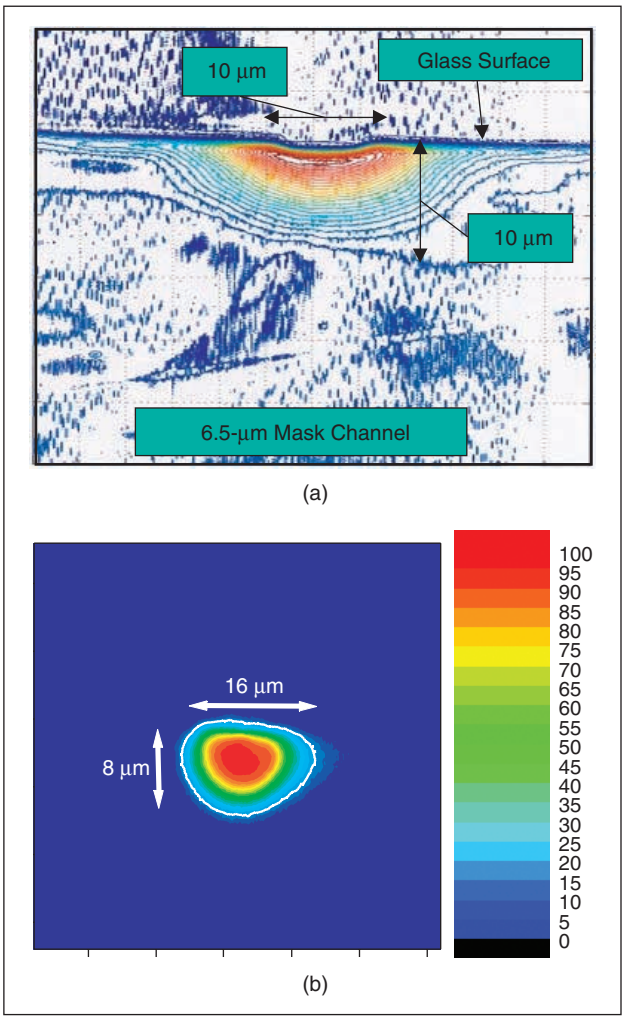

2. (a) Refracted ray scan showing end-on view of channel waveguide index contrast. From blue to red is a contrast of $\Delta n = 0.008$. (b) A near-field scan showing end-on view of the transmitted intensity through a channel waveguide at 1.55 µm. The mode is 8 µm in the vertical dimension and 16 µm wide at the $1/e^2$ intensity level (white contour).

laser and amplifier applications. In *ion exchange,* ions (e.g., Na^+) within the substrate are exchanged for ions (e.g., K^+, Ag^+) contained in a salt melt (e.g., KNO_3, $AgNO_3$) [1]. The ion exchange process is sometimes accelerated with the use of an electrical potential across the glass in a field-assisted ion exchange. Field-assisted ion exchange is useful in producing buried waveguides. In *laser photo-writing*, a tightly focused laser beam of high-peak power can change the refractive index in doped and undoped silicate glass [2]–[4]. This method has been used to "photo-write" waveguides and other refractive index features. *Rare-earth-doped film deposition* is performed through a variety of methods, including RF sputtering [5], [6], ion-implantation [7], plasma-enhanced chemical vapor deposition [8], flame hydrolysis [9], and sol-gel deposition [10]. This article will focus solely on thermally assisted ion exchange as a fabrication method for making optical waveguides.

Using the ion exchange method for fabricating optical waveguide lasers and amplifiers places a number of important constraints on the material used for the device. The material must contain species suitable for ion exchange (e.g., Na^+). The substrate must also be chemically durable to withstand the chemistry employed (e.g., aluminum acid etching) during standard lithographic processing for mask preparation and able to withstand the high temperature (375 °C) associated with thermal ion exchange processing. Obviously, the material must be doped with sufficient levels of active, rare-earth elements to provide gain when pumped by an external laser. The doping level of the rare-earth elements should be as high as possible (avoiding the effects of high-concentration quenching) to allow for the reduction of laser and amplifier cavity lengths. IOG-1 phosphate glass from Schott Glass Technologies is the substrate that we use for making channel waveguides, because IOG-1 meets all of these material requirements. (IOG-1 laser glass, Schott Glass Technologies, Inc., Duryea, Pennsylvania. The IOG-1 trade name is used only to allow the reader to reproduce the experiment and does not imply endorsement by the National Institute of Standards and Technology.) This laser glass contains Na^+, making it suitable for ion exchange, aluminum for chemical durability, and a mixture of active (Er and Yb) and passive (lanthanum) rare-earth elements to allow the active element doping concentration to be tailored without altering the base glass composition. In a typical waveguide laser application the concentrations of Yb and Er are 4×10^{20} ions/cm^3 and 1×10^{20} ions/cm^3, respectively, yielding a 4:1 Yb-to-Er ratio. Yb is added as a sensitizing ion to enhance pump laser absorption; this effectively increases the population inversion of the Er in the waveguide. In addition, phosphate-based glass has been shown to be superior for waveguide applications due to its thermal and mechanical stability [1].

Waveguide mask preparation starts with the deposition of a metal layer (e.g., 200 nm thick aluminum or titanium) to form an ion diffusion barrier. The diffusion mask is then etched across the length of the substrate with standard lithographic techniques. The channels in the mask that define the planar waveguides are typically 3–8 μm wide. The masked glass plates are then loaded into a sealed crucible containing potassium nitrate (KNO_3) salt. The crucible is heated to 375 °C, and the masked glass plates are submerged in the molten salt for four hours. During this time, K^+ ions diffuse into the glass and exchange with Na^+ ions in the original glass. This process is illustrated schematically in Figure 1.

After the thermal ion exchange is completed, the glass plates are diced into pieces suitable for lasers (typical length = 1.5–2.5 cm), the end faces of the waveguides are polished to optical quality, and the diffusion mask is removed by an acid etch. The waveguide index and mode profile can then be mapped with techniques, such as refracted ray near-field scanning [11] [Figure 2(a)] or near-field imaging [Figure 2(b)]. The refracted ray experiments measure a contrast in refractive index of $\Delta n = 0.008$ between the unexchanged substrate and the

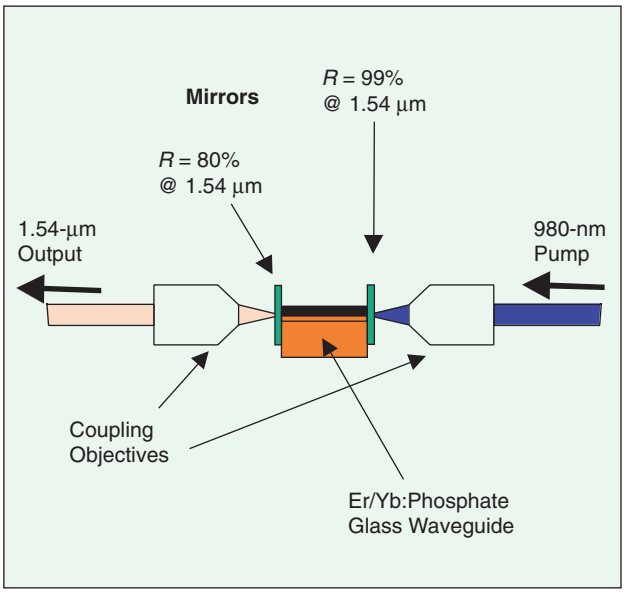

3. An FP waveguide laser schematic. This laser operates at 1,540 nm when pumped by a 980-nm source.

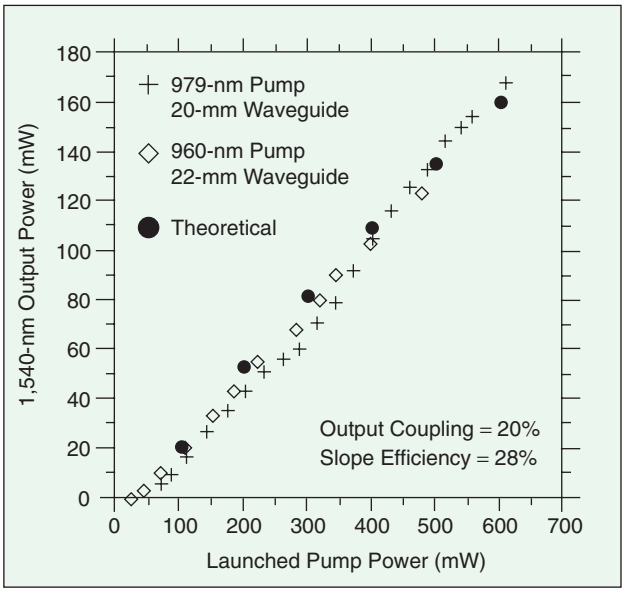

4. Er/Yb FP waveguide laser output power at 1,540 nm versus launched pump power at 960 nm and 979 nm. Lasing threshold achieved with 45mW of coupled pump at 979 nm.

waveguide. The near-field imaging provides information about the mode profile of the waveguide. The waveguides formed with mask channels up to 6 μm wide tend to be single-mode at 1,540 nm after the four-hour ion exchange. The mode profile is slightly elliptical, with typical dimensions of 6.5 μm $\times$ 7.5 μm in the vertical and horizontal dimensions, respectively. The waveguides will have a more circular, less elliptical mode profile if they are buried into the glass substrate by means of a field-assisted ion exchange. Burying the waveguides can provide other benefits as well (e.g., lowering loss of the waveguides and lowering noise in mode-locked applications).

Fabry-Perot Laser Performance

Once a broadband 1,540-nm mirror is attached to each end of the glass, the polished Er/Yb codoped waveguides easily form a simple Fabry-Perot (FP) laser cavity (Figure 3). The mirrors can be held fixed against the ends of the waveguides with index matching oil between the mirror and waveguide faces. In a typical experiment, one of the mirrors is a high reflector and the other is a 20% output coupler. Typical waveguide cavity lengths are 2–2.5 cm. The FP laser cavity is pumped either with a tunable Ti:Sapphire or diode laser ($\lambda \approx 980$ nm). The pump light may be coupled into the waveguide with microscope objectives. In this laser configuration, the waveguide coupling efficiency of the pump laser light is typically 40–50%. Waveguide lasers are also easily fiber-coupled for fiber-based applications using standard fiber alignment and bonding procedures. These lasers have output power slope efficiencies approaching 30% and output power up to 170 mW when a 20% output coupler is used [Figure 4(a)] [1]. The output of the FP laser also exhibits multiple longitudinal modes. Without the end mirrors these lasers make excellent amplifiers for 1.55-μm telecommunications applications. Several companies are currently utilizing this technology to build amplifiers with small-signal gain as high as 24 dB and power saturation at 10 dBm [12], [13]. The subject of waveguide amplifiers is beyond the scope of this article.

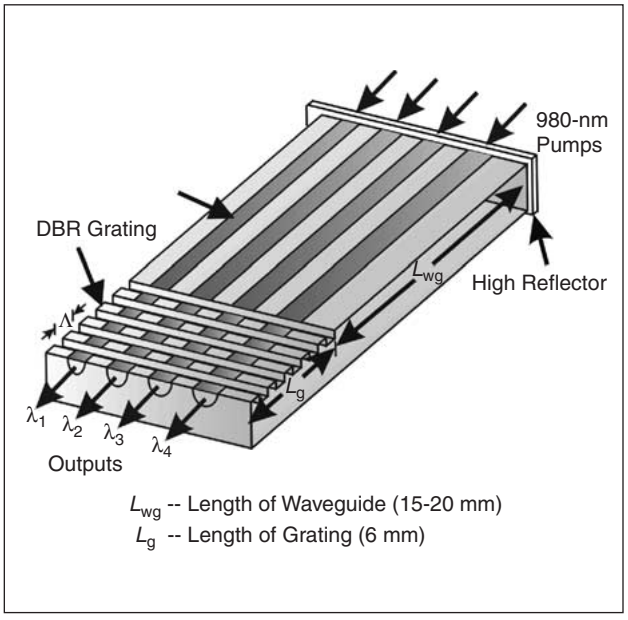

5. A DBR waveguide laser. DBR grating is etched into the top surface of the channel waveguide. Varying the width of the channels varies the local index of the waveguide and, therefore, the single-frequency output wavelength for each waveguide [see (1)].

Single-Frequency Er/Yb Waveguide Lasers

Single-frequency glass waveguide lasers operating near 1,550 nm have a number of advantages over single-frequency semiconductor lasers. The main advantage is narrower linewidth. Semiconductor lasers are reliable, come in small packages, provide high output power, and are relatively easy to use; therefore, these lasers have historically been heavily used in telecommunications applications. Unfortunately, the spectral output of these lasers is broad (1–3 MHz), although it may be narrowed to tens of kilohertz by adding the extra complexity of an extended-cavity configuration [14], [15]. Fast spontaneous emission events in semiconductors (nanosecond timescale) drive the gain of the laser away from equilibrium, which causes small changes in the local refractive index of the medium and a concomitant broadening of the laser line [16]. This fact makes semiconductor lasers unsuitable for applications such as remote sensing and metrology, where a linewidth less than 100 kHz is desirable.

The single-frequency waveguide distributed Bragg reflector (DBR) laser also outperforms fiber lasers. Most single-frequency fiber lasers are able to achieve narrow linewidths less than 100 kHz [17], [18]. However, the output power of these lasers is typically less than 10 mW because the Er/Yb doping level available in silica fiber limits the gain of the laser. A narrow linewidth less than 10 kHz has been demonstrated with a fiber ring laser, but the maximum output power was only 1.3 mW [17], [18]. Also, fiber ring lasers can be difficult to use and lack reliability for many industrial applications. Waveguide lasers have a distinct advantage over fiber lasers in that they have much higher dopant concentrations of Er and Yb and, therefore, have higher gain in a much more compact package. As we shall see, this provides much higher output power without sacrificing narrow linewidth.

The multimode FP laser can be made into a single-frequency laser when a DBR is etched into the top surface of one end of the waveguide (Figure 5). The DBR acts as the output coupler of the laser, and the period of the DBR grating determines the frequency of the laser oscillation. The grating pattern is made using holographic exposure of a thin layer (500 nm) of photoresist. The period (Λ) of the DBR is tailored to the desired laser output wavelength (λ_0) during the holographic exposure using the exposure angle (θ_{exp}), and by considering the local effective index (N_{eff}) of the waveguide mode and holographic exposure wavelength (λ_{exp}) according to:

$$\Lambda = \frac{\lambda_0}{2N_{\text{eff}}} = \frac{\lambda_{\text{exp}}}{2n_{\text{air}}\sin\theta_{\text{exp}}} \qquad (1)$$

where n_{air} is the index of air. Once the photoresist is developed, the grating pattern is transferred into the glass surface of the waveguide by Ar^+ ion etching. Channel waveguides

with different widths will have a slightly different local index (N_{eff}), and will, therefore, oscillate at slightly different wavelengths for a given DBR period. This is a convenient way to obtain multiple wavelengths from a single glass chip.

The DBR waveguide can be made into a laser with the addition of a high-reflectivity mirror. Such lasers have demonstrated output powers of 20 mW when pumped by modest 980-nm diode lasers and reach threshold with 45 mW of coupled pump power [1]. The typical slope efficiency for these DBR waveguide lasers is 20%. Output power approaching 100 mW can be

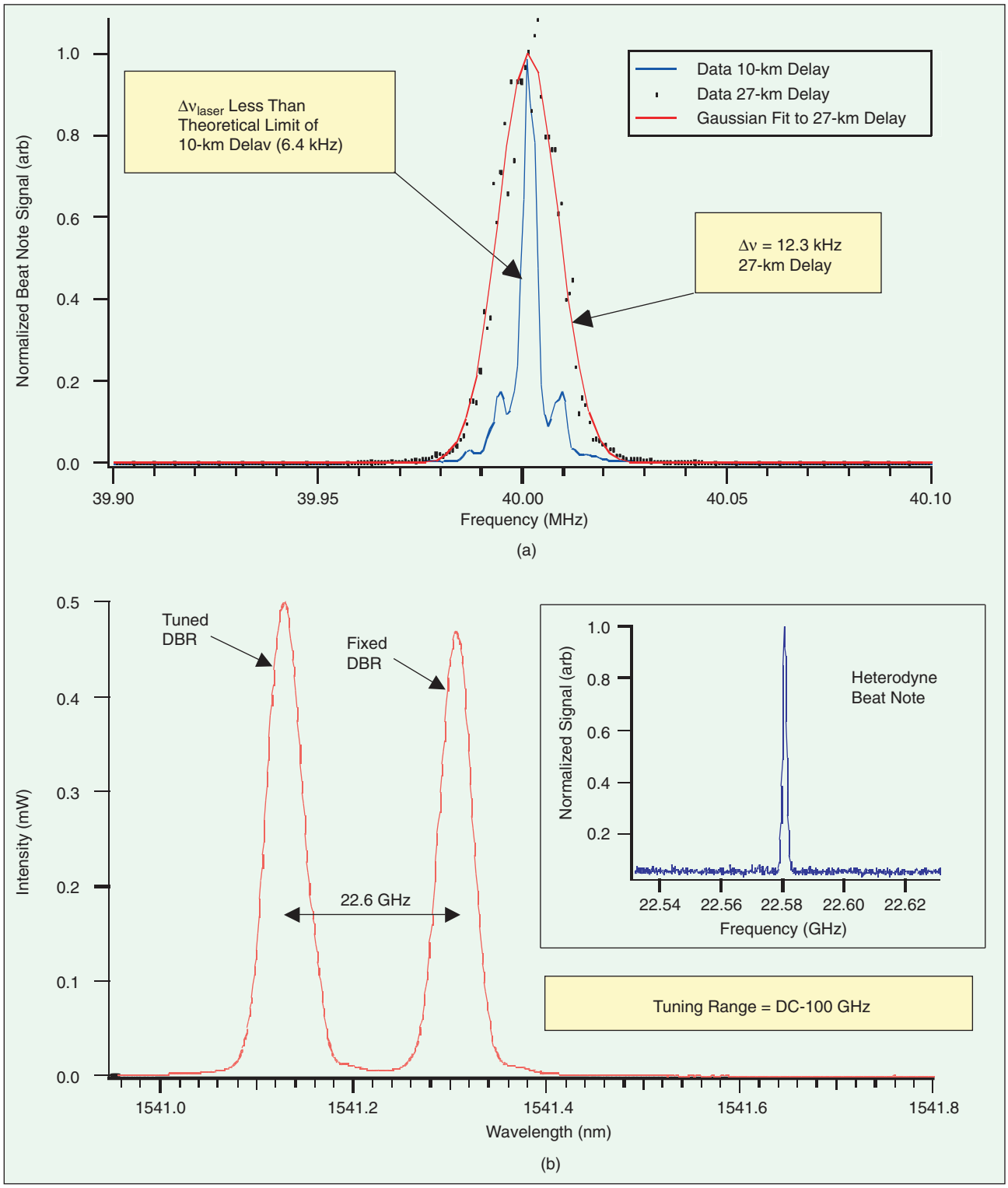

6. (a) The delayed self-heterodyne beat-note frequency spectrum for a typical DBR waveguide laser. The fiber delays are 10 and 27 km, and the AOM frequency shift is 40 MHz. (b) A spectrum of two DBR waveguide lasers and their heterodyne beat-note (inset) formed by mixing their output on a fast photo-detector. The beat-note tuning range is dc–100 GHz with temperature tuning of one of the DBR lasers.

obtained from these lasers with higher coupled pump power near 500 mW [1]. This is still below the saturation level for the dopant concentration in the waveguide. It is possible to measure the reflectivity of the etched DBR grating with the analysis of Rigrod [19]. These devices typically have a grating reflectivity of 65–70%. This parameter can be tailored to maximize the output power for other dopant species by changing the length or etch depth of the grating.

The linewidth of the laser can be measured with a standard delayed self-heterodyne technique [20]. Part of the output of the laser is frequency shifted with an acousto-optic modulator (AOM). After a fiber delay, the frequency-shifted light is recombined with the original light from the laser to produce a beat-note at the AOM operating frequency. As long as the fiber delay is longer than the coherence time of the laser, the frequency width of the obtained beat-note will give an accurate measurement of the linewidth of the laser. A typical delayed self-heterodyne spectrum is shown in Figure 6(a) for two fiber delays and an AOM frequency of 40 MHz. The frequency power spectrum obtained with a 10-km delay shows oscillations due to phase coherence between the frequency shifted light and the delayed light from the laser. These oscillations indicate that the linewidth of the laser is below the theoretical resolution of this delay ($\Delta\nu_{\text{theoretical}} = 6.4$ kHz). The period of the oscillations is equal to the inverse of the fiber delay time [21], [22]. The spectrum obtained with a 27-km delay has a Gaussian lineshape with a width of 12.3 kHz[$\Delta\nu =$ full width at half maximum (FWHM)/$\sqrt{2}$]. A Lorentzian lineshape is expected for the frequency power spectrum of the laser. This is because the fluctuations in the optical field should be due to spontaneous-emission events in the laser. The Gaussian lineshape in the power spectrum for the 27-km delay length indicates that the beat-note is broadened by the effect of 1/*f* noise in the detection system [23]. The use of a longer fiber delay allows the lower frequencies in the noise spectrum of the laser and detection system to have an impact on the width of the beat-note obtained in the measurement. Therefore, this analysis sets an upper bound on the linewidth of the laser at 6.4 kHz, the theoretical resolution of the 10-km delay. The results of these experiments show that the linewidth of this simple, monolithic DBR waveguide laser is comparable to that obtained with complex fiber ring lasers and a factor of 100 less than standard semiconductor lasers.

It is important that single-frequency lasers be tunable for many industrial applications. The frequency spacing is 50 GHz (0.39 nm) in the 81-channel International Telecommunications Union (ITU) grid in the C-band. The ability to tune between lines in the ITU grid is a valuable property for a laser used in wavelength division muliplexed (WDM). Temperature tuning the monolithic waveguide DBR laser has shown a tuning range of 0.8 nm [1]. Strain tuning may provide more tuning range. The C-band in DWDM covers 1,528–1,561 nm. An Er/Yb codoped waveguide laser with tunable external cavity grating can tune 40 nm from 1,525–1,565 nm [1]. Other telecommunications wavelengths can be covered by changing the active rare-earth element in the glass.

Single-frequency lasers, when tunable, can also be used to generate optical RF and microwave signals of arbitrary frequency. This is done with the optical heterodyne technique by using two lasers with a frequency difference equal to that of the RF or microwave signal desired [Figure 6(b)]. Tuning the relative separation of two 1,540-nm lasers from 0–0.8 nm yields an electrical signal range of dc to 100 GHz. A number of companies currently sell turnkey, diode laser versions of this device. This technology is raising interest for all optical RF and microwave signal generation, distribution, and processing, and also wide-bandwidth detector characterization. The linewidth of the beat-note generated from this technique (and, consequently, the resolution of the electrical signal) is only as narrow as the linewidth of the laser sources used. Therefore, narrow linewidth sources are important if precise RF and microwave signals are desired.

Passively Mode-Locked Waveguide Lasers

High-data-rate communications systems and high-speed photonic digital-to-analog conversion can benefit greatly from a compact source of short optical pulses with low noise and little chirp [24], [25]. Mode-locked waveguide lasers can provide low-jitter picosecond pulses at repetition rates exceeding 1 GHz. It is important to note that these high repetition rates are achieved with mode locking at the fundamental round-trip frequency of the laser cavity (fundamental mode locking). Fiber lasers must be meters long to achieve the gains possible

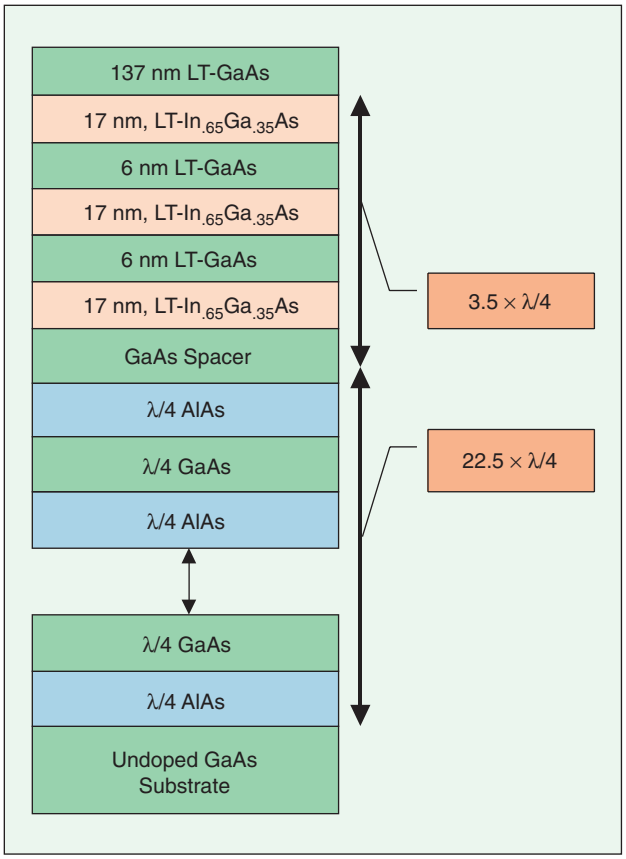

7. The structure of a semiconductor saturable absorber mirror (SESAM). The SESAM consists of low-temperature-grown (LT) InGaAs quantum wells on top of alternating AlAs and GaAs quarter-wave mirror layers.

in a waveguide laser of a few centimeters in length. To achieve gigahertz repetition rates, fiber lasers are mode-locked at some higher harmonic of the laser cavity's fundamental round-trip frequency (harmonic-mode locking). Multiple pulses circulate within a harmonically mode-locked laser, and these pulses can generate super-mode or pattern noise problems [26]. This pattern noise is avoided in fundamentally mode-locked waveguide lasers. Passively mode locking waveguide lasers offer advantages in simplicity and reduced intracavity loss (or higher cavity Q). No high-speed active modulator, with its associated insertion loss, is required to mode lock the laser. Instead, a nonlinear element is placed at

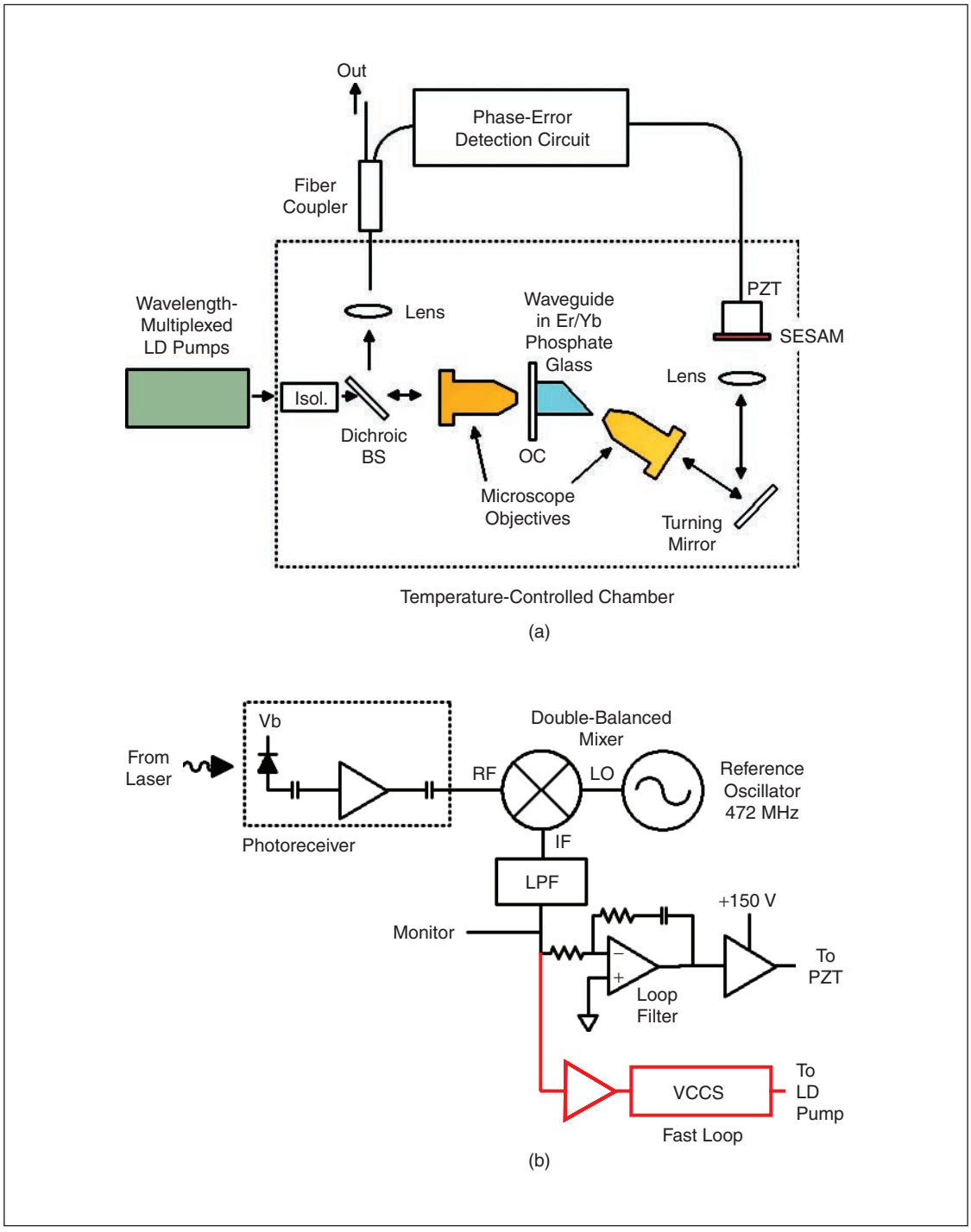

8. (a) The schematic of a mode-locked waveguide laser in an extended cavity configuration including active cavity circuitry: BS = beam splitter, OC = output coupler, PZT = piezo-electric transducer, LD = laser diode, SESAM = semiconductor saturable absorber mirror. (b) Mode-locked laser active cavity control circuitry with high-speed loop highlighted in red: V_b = bias voltage, RF = radio frequency from mode-locked pulse train, LO = local crystal oscillator, IF = intermediate frequency, LPF = low-pass filter, PZT = piezo-electric transducer, VCCS = voltage-controlled current source.

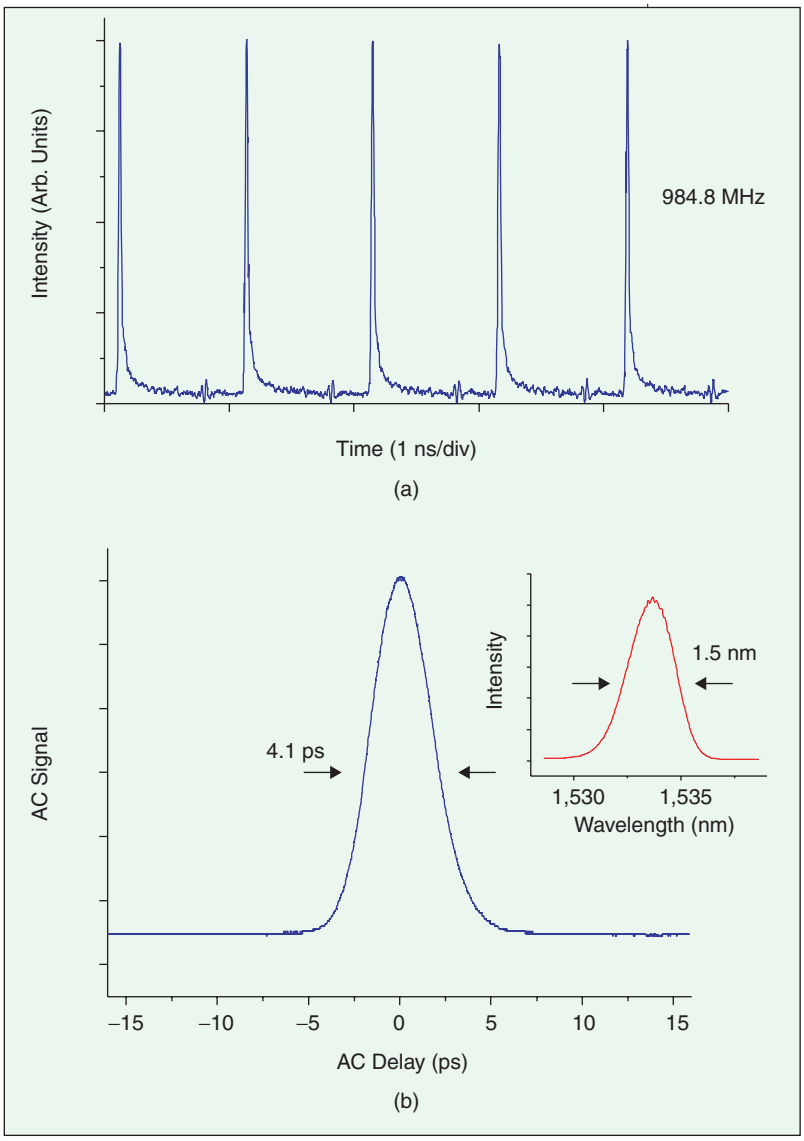

9. (a) The pulse train for mode-locked operation at repetition rate of 984.8 MHz. (b) Autocorrelation and bandwidth (inset) of laser pulses. The time-bandwidth product is 0.58 for these data when a Be-doped SESAM is used.

one end of the laser cavity to favor the formation of intense pulses [27]. In our case, the nonlinear element is a semiconductor saturable absorber mirror (SESAM) whose reflectivity increases with incident light intensity. This encourages the formation of mode-locked pulses from the initial intensity noise that exists within the laser cavity. In addition, passively mode-locked lasers can be actively phase locked to a stable electronic reference oscillator for applications similar to those mentioned above where an external clock is often provided.

The Mode-Locked Laser Setup

The heart of the passively mode-locked waveguide laser is the same high-gain Er/Yb codoped waveguide device described above for the FP laser. However, for the mode-locked laser, one of the end mirrors is replaced with a SESAM (Figure 7). Low-temperature-grown semiconductor quantum wells in the upper layers of the SESAM serve as a saturable absorber. Pulses that bleach these quantum well layers are reflected with low loss by a Bragg mirror stack that completes the SESAM structure. The composition of the semiconductor quantum wells is tailored for the wavelength of the mode-locked laser. For a lasing wavelength near 1,550 nm, low-temperature-grown InGaAs or InP are the materials of choice for quantum wells.

A typical extended cavity waveguide laser in a passively mode-locked configuration is shown in Figure 8(a), and a feedback circuit for cavity-length control is shown in Figure 8(b). During mode-locked operation, this laser produces average power of 4.5 mW, with 180 mW of coupled pump power at 977 nm from two wavelength-multiplexed laser diodes [28]. Average output power of 20 mW is observed when pumped with a pump laser system having higher power [29]. The mode-locked pulse train is shown in Figure 9(a) for a repetition rate of 984.8 MHz. Repetition rates exceeding 1 GHz have been observed with this system. The laser produces 6-ps pulses (Gaussian shape autocorrelation FWHM = 8.5 ps) with a bandwidth of 0.65 nm centered at 1,533.5 nm without any compensation for the cavity dispersion. The presence of a slight pulse chirp is indicated by the time-bandwidth product $\Delta\nu\Delta t = 0.5$. Pulsewidths as low as 4.1 ps FWHM with 1.5 nm of bandwidth ($\Delta\nu\Delta t = 0.58$) are shown in Figure 9(b) using beryllium-doped, low-temperature-grown InGaAs quantum wells in the SESAM [28], [30]. This quantum well material has a faster saturation recovery time.

Jitter Control

Mode-locked lasers can produce pulse trains with extremely regular pulse intervals or low pulse-to-pulse timing jitter. Lower intra-cavity loss (or higher cavity Q) is advantageous here, for it enables increased photon lifetimes, less need for laser gain [thus, less amplified-spontaneous-emission (ASE) noise], and, ultimately, lower timing jitter. Low-jitter sources improve the performance of high-data-rate communications systems by improving bit-error rates due to data pulses leaving their temporal bit slots. They can also reduce timing errors in A-D conversion systems, thus improving signal-to-noise ratios. As mentioned above, a passively mode-locked laser has no (lossy) active modulator driven by an external clock, however, the laser's repetition rate can still be referenced to a system clock. This is accomplished by referencing the cavity's repetition frequency to an external oscillator through active cavity-length control [31], [32]. Fortunately,

many of the environmental noise sources that affect laser cavity length (thus changing pulse-to-pulse timing jitter) occur at relatively low frequencies (less than 10 kHz) and can be removed with a feedback loop that has a modest frequency response. Furthermore, unlike semiconductor lasers, the relaxation oscillations for these lasers occur at frequencies below 500 kHz, thus, the additional noise from these oscillations can also be removed with a readily achievable feedback control loop. Figure 8(b) shows the feedback circuit used to accomplish cavity-length control. A double balanced mixer serves as a phase detector that produces an error signal proportional to the phase difference of signals from the mode-locked laser and a reference oscillator. The filtered and amplified error signal changes the cavity length of the laser by changing the voltage across a piezo-electric transducer (PZT) that moves the SESAM at one end of the cavity. A phase lock is achieved when the phase difference between the mode-locked laser and the reference oscillator (thus, the frequency difference) is zero. The performance of such a lock can be determined by measuring the single-sideband (SSB) phase noise of the mode-locked laser with and without lock. Figure 10 shows the SSB phase noise for a waveguide laser fundamentally mode-locked at 472 MHz with and without lock to a reference oscillator. These phase-noise measurements were made with the phase-detector method [33]. Root-mean-square (rms) timing jitter $\tau_{j,\mathrm{rms}}$, given the laser repetition frequency f_R, is calculated for the Fouier or offset frequency range of interest $f_{\min}$ to $f_{\max}$ over the SSB phase noise $\mathcal{L}$ per [33]:

$$\tau_{j,\,\mathrm{rms}} = \frac{1}{2\pi f_R}\sqrt{2\int_{f_{\min}}^{f_{\max}} \mathcal{L}\, df} \qquad (2)$$

For this laser, the rms jitter is more than 1.8 ps (100 Hz–10 MHz) without lock and 83 fs (100 Hz–10 MHz) with lock. Phase noise at higher offset frequencies (up to ~1 MHz) can be removed with the addition of a faster feedback loop that modulates pump power through control of the laser diode pump current [see red highlight in Figure 8(b)]. Modulation of the pump power enables modulation of the laser's optical length through pump-induced changes in atomic dispersion [34]. This technique reduced timing jitter in an extended-cavity waveguide laser having a 750 MHz repetition rate to 14.4 fs over a complete offset frequency range of 10 Hz to 375 MHz, the Nyquist frequency of this source [35]. Such ultralow jitter performance shows great promise for applications in high-bit-rate optical time-domain communications, photonic A-D conversion, and optical clock distribution. In addition, shorter monolithic lasers are possible with SESAMs directly butted to the waveguide end faces. These designs should prove both compact and robust to environmental noise and be particularly well suited for integration into both mobile and fixed optical-fiber-based systems.

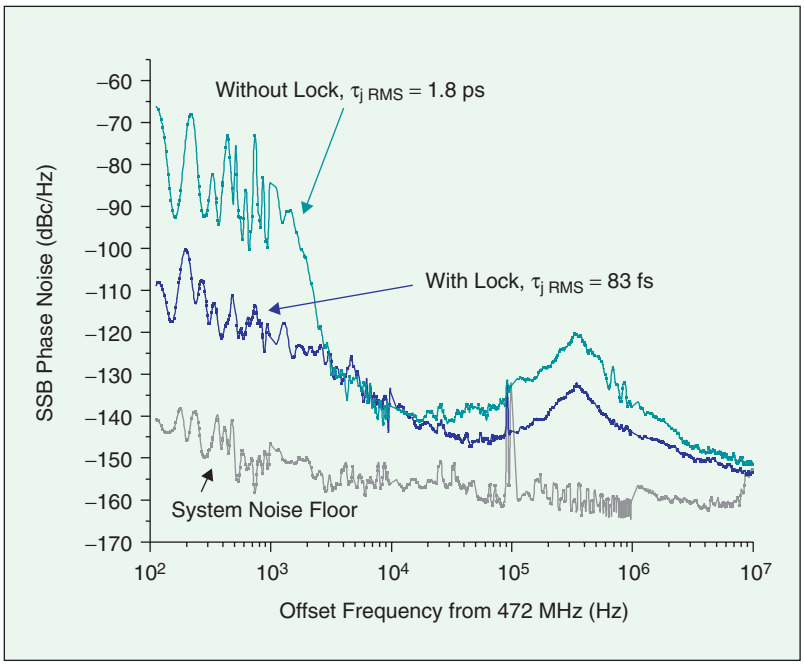

10. Single-sideband (SSB) phase noise measurement from 100 Hz to 10 MHz. Active cavity lock to reference oscillator reduces SSB phase noise and pulse-to-pulse jitter.

Conclusion

Glass waveguide lasers will fill an important niche as optical sources in communication, RF photonics, and optical metrology. This is primarily because waveguide lasers benefit from compact size, low noise, relatively high output powers, long upper-state lifetimes, and simple integration with optical-fiber-based systems. Although we do not expect waveguide lasers and amplifiers to ever supplant fiber and semiconductor lasers and amplifiers in every possible communications application, waveguide lasers have a number of advantages over traditional lasers for these uses. Single-frequency waveguide lasers provide narrow linewidth and high output power in a compact, monolithic package. The narrow linewidth is an important advantage over standard semiconductor lasers, and the compact size makes single-frequency waveguide lasers better suited than fiber lasers or extended-cavity semiconductor lasers for many applications. Mode-locked waveguide lasers provide short pulses with ultralow jitter and high average power. The effects of super-mode and pattern noise found in harmonically mode-locked fiber lasers are avoided with fundamentally mode-locked waveguide lasers. The long upper-state lifetime of the Er/Yb lasing transition allows mode-locked waveguide lasers to operate at repetition rates unavailable in mode-locked semiconductor lasers. Finally, waveguide lasers are easily integrated into optical-fiber-based systems, which is an important advantage over bulk lasers.

Berton E. Callicoatt, John B. Schlager, Robert K. Hickernell, Richard P. Mirin, and *Norman A. Sanford* were all with the National Institute of Standards and Technology in Boulder, Colorado when this work was performed. Dr. Callicoatt is now with Coherent Technologies, Inc., Louisville, Colorado. E-mail: schlager@boulder.nist.gov.

References

[1] D.L. Veasey, D.S. Funk, P.M. Peters, N.A. Sanford, G.E. Obarski, N. Fontaine, M. Young, A.P. Peskin, W.-C. Liu, S.N. Houde-Walter, and J.S. Hayden, "Yb/Er-co-doped and Yb-doped waveguide lasers in phosphate glass," *J. Non-Cryst. Solids,* vol. 263–264, pp. 369–381, Mar. 1, 2000.

[2] K.M. Davis, K. Miura, N. Sugimoto, and K. Hirao, "Writing waveguides in glass with a femtosecond laser," *Opt. Lett.,* vol. 21, pp. 1729–1731, Nov. 1, 1996.

[3] Y. Sikorski, A.A. Said, P. Bado, R. Maynard, C. Florea, and K.A. Winick, "Optical waveguide amplifier in Nd-doped glass written with near-IR femtosecond laser pulses," *Electron. Lett*., vol. 36, pp. 226–227, Feb. 3, 2000.

[4] C.B. Schaffer, A. Brodeur, J.F. Garcia, and E. Mazur, "Micromachining bulk glass by use of femtosecond laser pulses with nanojoule energy," *Opt. Lett*., vol. 26, pp. 93–95, Jan. 15. 2001.

[5] J. Shmulovich, A. Wong, Y.H. Wong, P.C. Becker, A.J. Bruce, and R. Adar, "Er^{3+} glass waveguide amplifier at 1.5 μm on silicon," *Electron. Lett*., vol. 28, pp. 1181–1182, June 18, 1992.

[6] Y.C. Yan, A.J. Faber, H. de Waal, P.G. Kik, and A. Polman, "Erbium-doped phosphate glass waveguide on silicon with 4.1 dB/cm gain at 1.535 μm," *Appl. Phys. Lett*., vol. 71, pp. 2922–2924, Nov. 17, 1997.

[7] G.N. van den Hoven, R.J.I.M. Koper, A. Polman, C. van Dam, J.W.M. van Uffelen, and M.K. Smit, "Net optical gain at 1.53 μm in Er-doped Al_2O_3 waveguides on silicon," *Appl. Phys. Lett*., vol. 68, pp. 1886–1888, Apr. 1, 1996.

[8] S. Guldberg-Kjaer, J. Hubner, M. Kristensen, C. Laurent-Lund, M.R. Poulsen, and M.W. Sckerl, "Planar waveguide laser in Er/Al-doped germanosilicate," *Electron. Lett*., vol. 35, pp. 302–303, Feb. 18, 1999.

[9] T. Kitagawa, K. Hattori, M. Shimizu, Y. Ohmori, and M. Kobayashi, "Guided-wave laser based on erbium-doped silica planar lightwave circuit," *Electron. Lett*., vol. 27, pp. 334–335, Feb. 14, 1991.

[10] M. Benatsou, B. Capoen, M. Bouazaoui, W. Tchana, and J.P. Vilcot, "Preparation and characterization of sol-gel derived Er^{3+}:Al_2O_3-SiO_2 planar waveguides," *Appl. Phys. Lett*., vol. 71, pp. 428–430, July 28, 1997.

[11] N.H. Fontaine, and M. Young, "Two-dimensional index profiling of fibers and waveguides," *Appl. Opt*., vol. 38, pp. 6836–6844, Nov. 1999.

[12] K.C. Reichmann, P.P. Iannone, M. Birk, N.J. Frigo, D. Barbier, C. Cassagnettes, T. Garret, A. Verlucco, S. Perrier, and J. Philipsen, "An eight-wavelength 160-km transparent metro WDM ring network featuring cascaded erbium-doped waveguide amplifiers," *IEEE Photon. Technol. Lett*., vol. 13, pp. 1130–1132, Oct. 2001.

[13] J. Bristow, "Waveguide amplifiers compensate passive optical component losses," *Laser Focus World*, vol. 38, pp. 101–104, June 2002.

[14] M. Okai, T. Tsuchiya, A. Takai, and N. Chinone, "Factors limiting the spectral linewidth of CPM-MQW-DFB lasers," *IEEE Photon. Technol. Lett*., vol. 4, pp. 526–528, June 1992.

[15] L. Hsu, A. Mooradian, and R.L. Aggarwal, "Spectral linewidth of a free-running continuous-wave single-frequency external cavity quantum-well InGaAs/AlGaAs Diode-laser," *Opt. Lett*., vol. 20, pp. 1788–1790, Sept. 1, 1995.

[16] G.P. Agrawal, and N.K. Dutta, *Semiconductor Lasers*, 2nd ed. New York: Van Nostrand, 1993, p. 269.

[17] K. Iwatsuki, H. Okamura, and M. Saruwatari, "Wavelength-tunable single-frequency and single-polarization Er-doped fiber-ring laser with 1.4 kHz linewidth," *Electron. Lett*., vol. 26, pp. 2033–2035, Nov. 22, 1990.

[18] J.T. Kringlebotn, P.R. Morkel, L. Reekie, J.L. Archambault, and D.N. Payne, "Efficient diode-pumped single-frequency erbium-ytterbium fiber laser," *IEEE Photon. Technol. Lett*., vol. 5, pp. 1162–1164, Oct. 1993.

[19] W.W. Rigrod, "Saturation effects in high-gain lasers," *J. Appl. Phys*., vol. 36, pp. 2487–2490, Aug. 1965.

[20] K. Kikuchi, A. Nakayama, and T. Okoshi, "Novel method for high-resolution measurement of laser output spectrum," *Electron. Lett*., vol. 16, pp. 630–631, July 31, 1980.

[21] H. Ludvigsen, M. Tossavainen, and M. Kaivola, "Laser linewidth measurements using self-homodyne detection with short delay," *Optics Comm*., vol. 155, pp. 180–186, Oct. 1, 1998.

[22] L.E. Richter, H.I. Mandelberg, M.S. Kruger, and P.A. McGrath, "Linewidth determination from self-heterodyne measurements with subcoherence delay times," *IEEE J. Quantum Electron*., vol. 22, pp. 2070–2074, Nov. 1986.

[23] L.B. Mercer, "1/f frequency noise effects on self-heterodyne linewidth measurements," *J. Lightwave Technol*., vol. 9, pp. 485–493, Apr. 1991.

[24] M. Saruwatari, "All optical signal processing for terabit/second optical transmission," *IEEE J. Select. Topics Quantum Electron.*, vol. 6, pp. 1363–1174, Nov.-Dec. 2000.

[25] P.W. Juodawlkis, J.C. Twichell, G.E. Betts, J.J. Hargreaves, R.D. Younger, J.L. Wasserman, F.J. O'Donnell, K.G. Ray, and R.C. Williamson, "Optically sampled analog-to-digital converters," *IEEE Trans. Microwave Theory Tech.*, vol. 49, pp. 1840–1853, Oct. 2001.

[26] X. Shan, and D.M. Spirit, "Novel method to suppress noise in harmonically mode-locked erbium fiber lasers," *Electron. Lett*., vol. 29, pp. 979–981, May 27, 1993.

[27] A.E. Siegman, *Lasers.* Mill Valley, CA: University Science Books, 1986, ch. 28.

[28] J.B. Schlager, B.E. Callicoatt, R.P. Mirin, and N.A. Sanford, "Passively mode-locked waveguide laser with low residual jitter," *IEEE Photon. Technol. Lett*., vol. 14, pp. 1351–1353, Sep. 2002.

[29] J.B. Schlager, B.E. Callicoatt, K.L. Silverman, R.P. Mirin, N.A. Sanford, and D.L. Veasey, "Mode-locked erbium/ytterbium co-doped waveguide laser," in *Proc. Conf. Lasers and Electro-Optics*, 2001, p. 87.

[30] P.W. Juodawlkis, D.T. McInturff, and S.E. Ralph, "Ultrafast carrier dynamics and optical nonlinearities of low-temperature-grown InGaAs/InAlAs multiple quantum wells," *Appl. Phys. Lett*., vol. 69, pp. 4062–4064, Dec. 23, 1996.

[31] D.R. Walker, D.W. Crust, W.E. Sleat, and W. Sibbett, "Reduction of phase noise in passively mode-locked lasers," *IEEE J. Quantum Electron*., vol. 28, pp. 289–296, Jan. 1992.

[32] M.J.W. Rodwell, D.M. Bloom, and K.J. Weingarten, "Subpicosecond laser timing stabilization," *IEEE J. Quantum Electron*., vol. 25, pp. 817–827, Apr. 1989.

[33] R.P. Scott, C. Langrock, and B.H. Kolner, "High-dynamic-range laser amplitude and phase noise measurement techniques," *IEEE J. Select. Topics Quantum Electron*., vol. 7, pp. 641–655, Jul.-Sept. 2001.

[34] S.C. Fleming and T.J. Whitely, "Measurement and analysis of pump-dependent refractive index and dispersion effects in erbium-doped fiber amplifiers," *IEEE J. Quantum Electron.*, vol. 32, pp. 1113–1121, July 1996.

[35] J.B. Schlager, B.C. Callicoatt, R.P. Mirin, N.A. Sanford, D.J. Jones, and J. Ye, "Passively mode-locked glass waveguide laser with 14 fs timing jitter," *Opt. Lett.*, to be published.

CD ■